THE DISTRIBUTION OF PLANETARY NEBULA NUCLEI IN THE LOG L-LOG T PLANE: INFERENCES FROM THEORY

R. A. Shaw
Lick Observatory
University of California
Santa Cruz, CA 95064

ABSTRACT. The expected distribution of planetary nebula nuclei (PNNs) on the log L-log T plane is calculated based upon modern stellar evolutionary theory, the initial mass function (IMF), and various assumptions concerning mass loss during post-main sequence evolution. The distribution is found to be insensitive to the assumed range of main-sequence progenitor mass, and to reasonable variations in the age and the star forming history of the galactic disk. Rather, the distribution is determined primarily by the heavy dependence of the evolution rate upon core mass, and secondarily upon the steepness of the IMF and other factors. The distribution is rather different than any found from observations, and probably reveals strong observational selection effects.

1. INTRODUCTION

Nearly a quarter-century has passed since the first serious attempts to study the evolution of the nuclei of planetary nebulae. The observational studies of O'Dell (1962, 1963), Harman and Seaton (1964), Seaton (1966), Schönberner (1981), Kaler (1983), and Heap and Augensen (1987) have traced the evolution of cool, luminous PNNs surrounded by dense, compact planetary nebulae, to temperatures exceeding 10^5 K, followed by sharply declining luminosities as the nebular shells expand and the stars contract to white dwarf dimensions. On the theoretical side, Paczyński (1971), Schönberner (1979), Iben (1982, 1984), and Wood and Faulkner (1986) have published evolutionary post-asymptotic giant branch (post-AGB) stellar models. They revealed the importance of shell nuclear burning in providing the source of luminosity and determining the rate of evolution through the PNN phase, as well as the extraordinary dependence of the evolutionary timescales upon PNN mass. Together, the observations and theory have established the planetary nuclei unambiguously as the link between the AGB and the white dwarfs. Iben and Renzini (1983, hereafter IR83) provide a general review of this subject.

Although our understanding of post-AGB stellar evolution has improved greatly, our ability to compare observational results with predictions from theory has not kept pace. Indeed, previous observational studies, such as those of Schönberner (1981), Kaler (1983), and Heap and Augensen (1987), have dealt only obliquely with the question of, *e.g.* the distribution of PNNs on the log L-log T plane that one would expect directly from theory. This paper will derive just such a theoretically-determined distribution, and compare it with those determined from

S. Torres-Peimbert (ed.), Planetary Nebulae, 473–480.

https://doi.org/10.1017/S007418090013904X Published online by Cambridge University Press

observations. The analysis will closely parallel that in Shaw, Truran, and Kaler (1984), and Shaw's (1985) doctoral dissertation.

2. CALCULATION OF THE LOG L-LOG T DISTRIBUTION

2.1. Theoretical Assumptions

The distribution expected from theory is possible to calculate in principle if the initial mass function (IMF), the relation between initial (main sequence) mass and post-AGB core mass, and the PNN evolution paths (including timescales) as a function of mass are all known. The following simplifying assumptions apply to this distribution calculation:

1. The adopted IMF is from Miller and Scalo (1979), which is well-known for stars less massive than 10 $M_\odot$. Furthermore, the slope of the IMF is assumed to be constant, although the effects of a slowly decreasing star formation rate are considered explicitly.
2. The function relating initial (main sequence) stellar mass to remnant (post-AGB) core mass is given by the nearly linear relation of Iben and Truran (1978), which is based upon Reimers' (1975) empirical formula for single, isolated stars. Here, stars up to 5 $M_\odot$ will produce PNNs, although a steeper linear function for stars up to 10 $M_\odot$ will be considered separately. In both cases it is assumed that no star less than 0.8 $M_\odot$ has evolved past the AGB in the lifetime of the galaxy, although a larger lower-limit will be adopted when a variation in galactic age is considered.
3. All stars that form degenerate cores less massive than the Chandrasekhar limit will illuminate a planetary nebula shell, or at least the fraction of those that do not does not change with PNN mass.
4. The evolutionary path through the log L-log T plane is uniquely defined by the PNN mass (see § 2.2 below), and each point in the log L-log T plane is intersected by one and only one evolution path (*i.e.* the evolution paths do not cross).
5. Only those stars that are passing through the PNN domain for the first time were included: those that suffer a post-AGB helium flash (see Iben 1984; Wood and Faulkner 1986) will be considered in § 4.1.
6. Finally, stars do not lose a significant amount of mass during the PNN phase, although the effect of the mass-loss process itself upon the rate of evolution will be discussed in § 4.1.

2.2. Adopted Stellar Models

Three specific post-AGB evolution models were adopted from Schönberner (1983): they have core masses of 0.546, 0.565, and 0.644 $M_\odot$. Two other models were taken from Paczyński (1971): they have core masses of 0.80 and 1.20 $M_\odot$. These models were chosen largely because they cover virtually the entire range of interest in mass, and because each investigator has provided a set of internally consistent evolution tracks that can be compared with the other investigator's models.

Unfortunately, this comparison reveals a major problem with the Paczyński models, namely the post-AGB helium flashes that result from an improper initial description of the structure of the AGB star (Schönberner 1981). Fortunately, as IR83 point out, a model PNN of a given, constant mass will always follow roughly the same path in the log L-log T plane, and the evolution timescales are not especially sensitive to details of the models. The discrepancy was resolved by comparing the 0.60 $M_\odot$ models and scaling those from Paczyński along the following guidelines: first, the luminosity of a remnant core that has just evolved off the AGB is approximately given by the linear relation (Schönberner 1983): $L_{PNN} = 6.0 \times 10^4 (M_{PNN} - 0.513)$; and second, the time required for the PNN to fade by 2.5 bolometric magnitudes after first ionizing the nebular shell scales roughly as $M_{PNN}^{-9.6}$ (IR83). This scaling also agrees well with the more recent models of Wood and Faulkner (1986) for higher PNN mass. In this same way, using the mass-radius relation for white dwarfs as an asymptote to the evolution path, the evolution track of an Chandrasekhar-limited PNN (*i.e.* at 1.4 $M_\odot$) was estimated.

2.3. The Domain

The calculation of the PNN distribution was done on a grid whose extent on the log L-log T plane extends over $1.6 < \log L/L_\odot < 4.8$, and $4.4 < \log T_{eff} < 6.1$. These limits were chosen partly for the availability of evolutionary models, and partly to correspond roughly to the domain over which the surrounding planetary nebula (PN) can be observed: the PNNs do not ionize the proto-planetary shell when they are cooler than $\log T_{eff} = 4.4$; the PNs are too distended to be detected easily after they expand for more than $\sim 30,000$ yr, which corresponds to about $\log L \geq 1.6$; and the other boundaries are set by the tracks of the most and least massive PNNs that pass through this domain (see § 2.1 and § 2.2).

The scheme was as follows: the PNNs were assumed to be forming at a constant rate, and the zero-point of the model timescales was adjusted such that $t = 0$ corresponds to the moment that the PNNs reach $\log T_{eff} = 4.4$. The domain was divided into grid intervals of 0.2 in log L, and 0.1 in log T. The evolution tracks were used to determine the mass track that passes through each grid point, and the time it takes a PNN on that track to evolve to that point. Each adjacent pair of grid points defined a boundary of a cell, within which the number of PNNs contained was calculated, according to the description of Fig. 1.

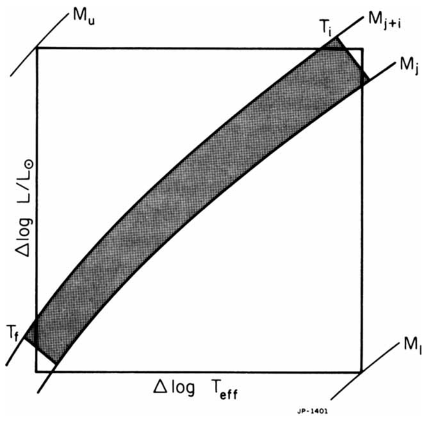

Fig. 1. Schematic representation of the calculation. Integration was performed over a strip spanning the evolution tracks M_j and M_{j+1} to yield the total number of PNNs in that mass interval. The product of that integral and the difference between times T_f and T_i (when the PNN leaves and enters the cell, respectively) yields the total number of PNNs in that strip. The total from each strip between M_l and M_u was summed and normalized such that the total from all cells in the PNN domain was unity.

https://doi.org/10.1017/S007418090013904X Published online by Cambridge University Press

3. THE DISTRIBUTIONS

The calculated distributions are listed in Fig. 2*a*, and shown as a contour plot in Fig. 2*b*, for the steady-state case. (A color representation of this distribution may be found in Kaler 1986.) This calculation, where progenitor masses between $0.8 < M_*/M_{PNN} < 5$ were included, will serve as a benchmark of comparison for the other calculations. The most striking feature in the figures is the tremendous range in relative number: about 8 orders of magnitude. This large range results from the great dependence of the evolution time-scales upon core mass and, hence, is also the greatest source of uncertainty in the calculations. The contours of constant PNN density are nearly coincident with lines of constant age (beyond $\log T_{eff} = 4.4$), and show that the vast majority of PNNs should be found along the lowest-mass evolution tracks, and at relatively low luminosity.

The next illustrative case is considered in Fig. 3, where progenitor stars up to 10 $M_\odot$ are assumed to produce PNNs. This change, though drastic in the broad context of stellar evolution, produces only a small change in the high mass portion of the log PNN distribution. And yet this subtle difference is not at all surprising in view of the steepness of the IMF—*i.e.* the number of stars formed in the 5 to 10 $M_\odot$ range is a very small fraction of the total number of PNN progenitors. The finite age of the galactic disk is addressed in the next calculation. Figure 4 shows the distribution where only those stars that evolve past the AGB within 1.0×10^{10} years (or $M_* > 1\ M_\odot$) are included. The disappearance of PNNs along the lowest-mass tracks is significant—reflecting the steepness of the IMF—but although the normalization for the distribution has changed, the relative numbers in each cell above the adjusted low-mass cut-off have remained constant. The next calculation includes an exponential decrease in the star formation rate, normalized to be a factor of 2 lower at present than at the birth of the galactic disk. This effect, shown in Fig. 5, is the smallest found in this study, and is naturally most pronounced in the high mass portion of the plane, due to the shorter stellar lifetimes.

4. INTERPRETATION

4.1. Lessons from Theory

Of the several conclusions that can be drawn from the distributions presented above, the surest is this: There is no hope of divining the range of PNN progenitor masses purely from considerations of an observed distribution in the log L-log T plane. Indeed, only ~1600 galactic PNs are known, which is far too few to examine a distribution which covers 8 orders of magnitude. There are other means of approaching the problem, however, which include a comparison of nebular He and CNO element abundances with those predicted by AGB dredge-up theory. Such a study by Kaler (1983), using the theory of Becker and Iben (1979, 1980), showed qualitative agreement. Another promising approach would be to use the abundances derived from stellar emission spectra for those PNNs with winds. Such an analysis may provide an interesting *ex post facto* radial probe of the nuclear burning and mixing processes in AGB stars, since the nebular shell and the subsequent winds came from different depths within the remnant AGB star.

IR83 note that the rate of evolution through the PNN domain is governed largely by the rate at which the star's fuel is depleted, be it through nuclear burning or mass-loss through a stellar wind. For typical mass-loss rates of 10^{-9}

https://doi.org/10.1017/S007418090013904X Published online by Cambridge University Press

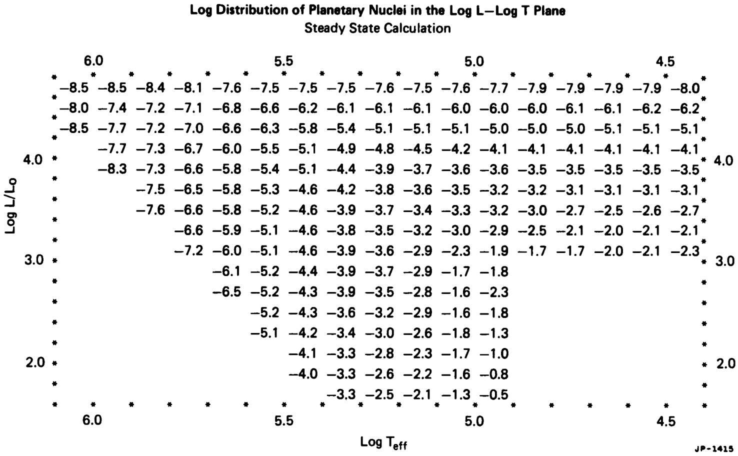

Fig. 2*a*. A two-dimensional histogram for the steady-state calculation showing the log of the relative number of PNNs in each cell on the log L-log T plane. This calculation includes the contribution from all progenitor stars in the mass range $0.8 < M_*/M_\odot < 5.0$.

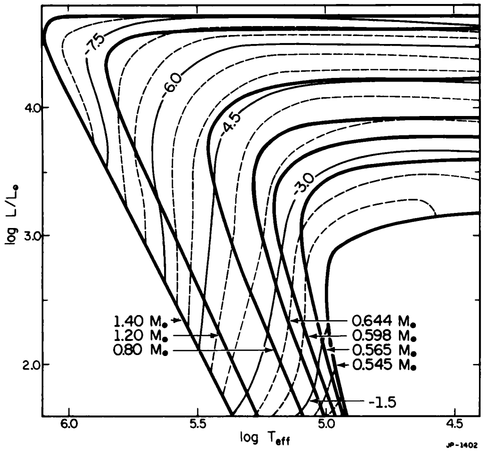

Fig. 2*b*. A contour plot of the log distribution presented in Fig. 2*a*. The intervals refer to the log of the relative number of PNNs expected to lie within each cell. Also shown are the adopted PNN evolution tracks (***heavy solid curves***): the 0.546, 0.565, 0.598 and 0.644 $M_\odot$ models are from Schönberner (1981), the 0.80, and 1.20 $M_\odot$ models are from Paczyński (1971, scaled), and the 1.4 $M_\odot$ model is from an estimate for the Chandrasekhar-limited case (see text).

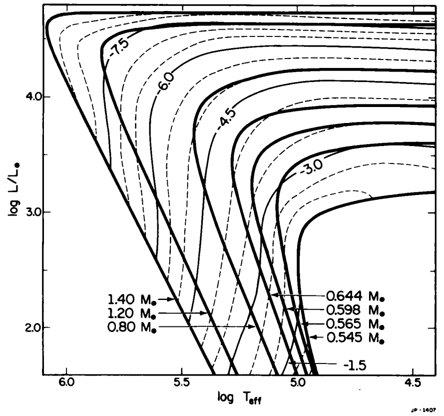

Fig. 3. Same as Fig. 2*b*, except that stars up to 10 $M_\odot$ are assumed to produce PNNs.

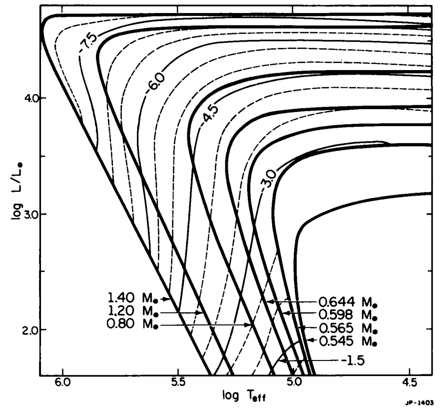

Fig. 4. Same as Fig. 2*b*, except that only those progenitor stars that have produced PNNs within the last 10 billion years are included.

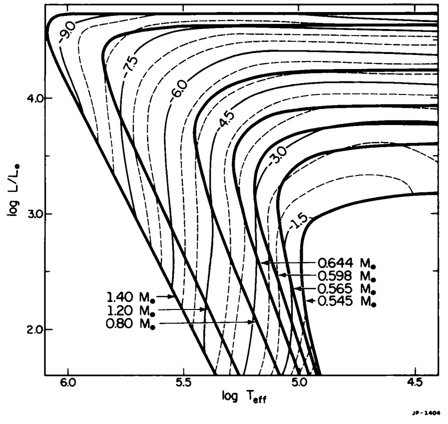

Fig. 5. Same as Fig. 2*b*, except that the SFR is assumed to have declined exponentially by a factor of 2 during the life of the galactic disk.

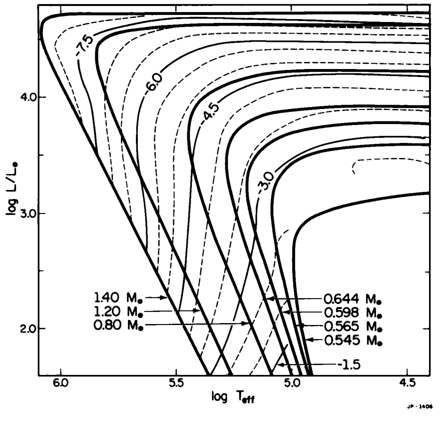

Fig. 6. Same as Fig. 2*b*, except that the PNNs are assumed to be undetectable after 30,000 yr.

to 10^{-7} $M_\odot$ yr^{-1}, and a typical hydrogen envelope mass of $\sim 10^{-3}$ to 10^{-4} $M_\odot$ (Iben 1984), a stellar wind could speed the PNN evolution by up to a factor of about 3. Although the explicit effect on the distribution of some fraction of PNNs (perhaps 50%) possessing winds was not calculated, it must compound the already high PNN density at low L, particularly for high mass PNNs if they preferentially engender high-velocity winds (see Wood and Faulkner 1986). On the other hand, if about 10% of all PNNs produce their luminosity through shell helium burning (Iben 1984), then somewhat more PNNs would be found at higher L (due to the slower evolution rate), near the lower-mass evolution tracks.

4.2. Observational Selection Effects

While the observed distributions cannot yield the PNN progenitor mass range directly, the theoretical distributions can reveal selection effects in the observed sample. In particular, the observed distributions of Schönberner (1981), Kaler (1983), and Heap and Augensen (1987) are not based upon a volume-complete sample, and do not match the broad features of that expected from theory. Furthermore, no such complete study has been done of those rare PNNs that are both extremely hot ($T_{eff} \geq 150,000$ K) *and* extremely luminous ($L \geq 10^3$ $L_\odot$).

Several effects may be operating to skew the observations. These include the systematic difficulties with the distance scale for young, optically thick PNs (Maciel and Pottasch 1980; Daub 1982); systematic contamination of the stellar continuum by the nebula in compact planetaries (Shaw and Kaler 1985); and the difficulty of discovering older, low surface brightness PNs due both to the drop in their emission measure as the shell expands, and to their propensity to lie in the galactic plane, where they suffer heavy interstellar extinction. The effect of aging nebular shells fading from view is shown in Fig. 6, where PNs older than 30,000 yr are assumed to be undetectable and are omitted. Although the contribution of low-mass PNNs at low L to the distribution is significantly smaller, the qualitative features are the same as in Fig. 2*b*, in that this distribution still predicts far more PNNs at low L than are seen observationally.

5. CONCLUSIONS AND FUTURE WORK

Clearly the theoretical distribution of PNNs on the log L-log T plane differs substantially from that determined from observations. It is probably also true that the theory for PNN evolution is far more secure than the observations, although an observationally complete, volume-limited sample of PNNs should be analyzed to understand fully the discrepancy. Those PNNs that have suffered a post-AGB helium shell flash (as is likely the case for A 30 and A 78: see Iben *et al.* 1983) must also be identified observationally, both to guide the theorists on the relative frequency of such events, and to allow for their effect on the observed distribution. It would be misleading to say that any one of the distributions calculated here on the basis of simplified stellar evolutionary theory represents the true distribution. Rather, the broad features of the distribution are presented to illustrate the nature of the discrepancy between observations and theory, and to suggest promising lines of investigation to resolve them.

Support for this research is acknowledged from NSF grants AST 80-23233 and 83-14415 to the Univ. of Illinois, and AST 86-11457 to the Univ. of California.

REFERENCES

Becker, S. A., and Iben, I. Jr. 1979, *Ap. J.*, **232**, 831.
Becker, S. A., and Iben, I. Jr. 1980, *Ap. J.*, **237**, 111.
Daub, C. T. 1982, *Ap. J.*, **260**, 612.
Harman and Seaton, M. 1964, *Ap. J.*, **140**, 824.
Heap, S. R., and Augensen, H. J. 1987, *Ap. J.*, **313**, 268.
Iben, I. Jr. 1984, *Ap. J.*, **277**, 333.
______. 1982, *Ap. J.*, **260**, 821.
Iben, I. Jr., Kaler, J. B., Truran, J. W., and Renzini, A. 1983, *Ap. J.*, **264**, 605.
Iben, I. Jr., and Renzini, A. 1983, *Ann. Rev. Astr. Ap.*, **21**, 271 (IR83).
Iben, I. Jr., and Truran, J. W. 1978, *Ap. J.*, **220**, 980.
Kaler, J. B. 1986, *Am. Scientist.*, **74**, 244.
______. 1985, *Ann. Rev. Astr. Ap.*, **23**, 89.
______. 1983, *Ap. J.*, **271**, 188.
Maciel, W. J., and Pottasch, S. R. 1980, *Astr. Ap.*, **88**, 1.
Miller, G. E., and Scalo, J. M. 1979, *Ap. J. Suppl.*, **41**, 513.
O'Dell, C. R. 1962, *Ap. J.*, **135**, 371.
______. 1963, *Ap. J.*, **138**, 67.
Paczyński, B. 1971, *Acta Astr.*, **21**, 417 (PZ).
Reimers, D. 1975, *Mem. Soc. R. Sci. Liege*, 6^e Ser. **8**, 369.
Schönberner, D. 1983, *Ap. J.*, **272**, 708.
______. 1981, *Astr. Ap.*, **103**, 119.
______. 1979, *Astr. Ap.*, **79**, 108.
Seaton, M. J. 1966, *M.N.R.A.S.*, **132**, 113.
Shaw, R. A. 1985, Ph. D. thesis, Univ. of Illinois.
Shaw, R. A., and Kaler, J. B. 1985, *Ap. J.*, **295**, 537.
Shaw, R. A., Truran, J. W., and Kaler, J. B. 1984, *Bull. A. A. S.*, **16**, 530.
Wood, P. R., and Faulkner, D. J. 1986, *Ap. J.*, **307**, 659.